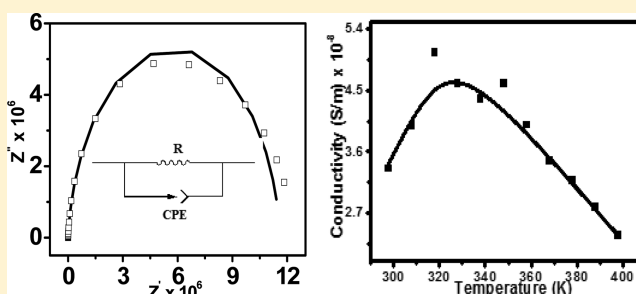


Nondestructive Characterization of Li^+ Ion-Doped Multifunctional Poly(vinylidene fluoride)-g-poly(dimethyl amino ethyl methacrylate) by Impedance Spectroscopy

Pratap Mukherjee, Aniruddha Kundu, Sanjoy Samanta, Somnath Roy, and Arun K. Nandi*

Polymer Science Unit, Indian Association for the Cultivation of Science, Jadavpur, Kolkata 700032, India

ABSTRACT: Poly(vinylidene fluoride) (PVDF)-graft-poly-(dimethyl amino ethyl methacrylate) (PDMAEMA) (PD copolymer) is produced via atom transfer radical polymerization from PVDF solution in *N*-methyl-2-pyrrolidone. PD copolymer is doped with 1% and 5% (w/w) Li^+ ion to produce PDLi1 and PDLi5 samples, respectively. In PD copolymer, the crystalline structure of PVDF changes from α polymorph to a mixture of α and β polymorph, and it transforms completely to piezoelectric β polymorph on doping with 1% (w/w) Li^+ ion. The impedance behavior of PVDF changes on grafting, and that of the PD graft copolymer also changes with increasing Li^+ ion dopant concentration. In the Nyquist plots, PVDF exhibits a straight line character, and a curvature has appeared in the PD graft copolymer; on doping the latter with Li^+ ion (1% w/w), the curvature increases and a semicircle is completed on 5% Li^+ doping. Fitting the data from the Z-view program, the Ohmic resistance of PDLi1 is found to be 78 M Ω having capacitance with constant phase element (CPE) = 1.38 nF while for the PDLi5 sample the resistance decreases to 16.1 M Ω with a small increase in CPE to 1.46 nF. The modulus plane plots for PDLi1 and PDLi5 samples also exhibit only one peak supporting the presence of only one equivalent resistance–capacitance circuit with constant phase element in both PDLi1 and PDLi5 samples. Both the impedance and modulus vs frequency plots of PDLi1 and PDLi5 samples exhibit a single Debye peak suggesting isotropic nature of the samples. For PVDF and PDMAEMA, ac-conductivity increases linearly with angular frequency, but in the case of PDLi1 and PDLi5 samples, it remains at first invariant in the frequency range $1\text{--}10^2$ Hz, and above 10^2 Hz, an increase in conductivity with frequency occurs obeying the double power law. In the temperature variation of conductivity, PVDF exhibits its typical insulating nature, and in the PD graft copolymer, the conductivity decreases with increase of temperature (metallic-like behavior) due to gradual breaking of supramolecular interaction. The temperature variation of ac-conductivity of the Li^+ -doped PD graft copolymer suggests that both the ionic and supramolecular contributions of conductivity operate; the former increases and the latter decreases with rise in temperature showing a maximum. The temperature-dependent FTIR spectra of PDLi1 and PDLi5 samples support the gradual breaking of supramolecular interactions with increase of temperature.



INTRODUCTION

In recent years, a great deal of research has been initiated to prepare multifunctional polymeric material, which can fulfill the specific demands of technologists in a single polymer.^{1–4} One way to make the commercial polymers multifunctional is grafting the main chain with reactive monomers. In a recent publication, we have reported the grafting of poly(dimethyl amino ethyl methacrylate) (PDMAEMA) on poly(vinylidene fluoride) (PVDF) (PD graft copolymer) backbone with a very high graft density so that supramolecular interactions become operative between $>\text{C}=\text{O}$ groups of PDMAEMA and $>\text{CF}_2$ groups of PVDF. It reduces the crystallinity of PVDF and induces super toughness and supergluing properties.² In this article, we are interested to investigate the impedance and conductivity change between PVDF and PD graft copolymer. The impedance property may originate from the supramolecular interactions forming numerous looplike structures in the PD graft copolymer.² The supramolecular interactions may disappear with increase of temperature, which can change the transport

property of the system. Also, by doping Li^+ ions to the PD graft copolymer, the impedance and conductivity property may change. So it would be interesting to ascertain the difference of electrical property, which would gradually generate on doping the PD graft copolymer with increasing amount of Li^+ ion concentration.

Polymer electrolytes find potential applications in the solid-state battery and in other electrochemical devices.^{5–11} Polyethylene oxide (PEO) doped with Li^+ ion is mainly used for this purpose. The oxygen atom of PEO acts as a coordination site to bind Li^+ ion via donor–acceptor interaction and Li^+ ion hops in different coordination sites within the amorphous phase.¹² In the PD graft copolymer,² the DMAEMA group can bind the Li^+ ion through the $>\text{N}$ atom of the dimethyl amino group and/or through the oxygen atom of the $>\text{C}=\text{O}$ group. As the

Received: October 5, 2012

Revised: January 8, 2013

Published: January 8, 2013

crystallinity of PD graft copolymer is lesser than that of the parent polymer PVDF, the Li^+ can hop through the amorphous zone of PD copolymer and is expected to exhibit an appreciable conductivity. This conductive polymeric hybrid may find a wide range of applications from electrochemical devices to solid-state battery because of its super toughness and supergluing properties.²

AC impedance spectroscopy has been used as a nondestructive testing tool for the study of electrolytic materials like ceramics, polymer electrolytes, etc.^{10–15} The impedance diagrams are usually interpreted based on equivalent circuit models that can give insight into the microstructural features of the material.¹⁶ One, or more than one, equivalent circuit is possible depending on the nature of bulk and grain boundaries present in the systems.¹³ Also the ac-conductivity vs frequency plot yields an insight into the conduction mechanism.^{9–16} In this article, we compare the impedance data of PVDF with that of PVDF-g-PDMAEMA (PD) polymer and also with those of the doped PD samples. The Li^+ -doped samples show the characteristic of an equivalent RC circuit, but it is absent in the undoped samples. The 5% Li^+ -doped sample exhibits an interesting behavior in the conductivity vs temperature plot; at lower temperature, an increase of conductivity occurs followed by a decrease of conductivity with temperature above 340 °C, and it might be compared with the semiconductor–metal transition.

■ EXPERIMENTAL SECTION

Samples. PVDF (Aldrich) has number average molecular weight $\bar{M}_n = 70\,000$, polydispersity index = 2.57, and head to head defect = 4.33 mol %. It was recrystallized from its 0.2% solution of acetophenone. The monomer DMAEMA (Acros Organics) was grafted on PVDF backbone by ATRP technique using cuprous chloride (CuCl) as a catalyst and 4,4'-dimethyl-2,2'-dipyridyl (DMDP) as a ligand in *N*-methyl-2-pyrrolidone (NMP) solvent according to the procedure reported earlier.² The polymerization was performed at 90 °C for 24 h. The polymer was precipitated in petroleum ether (60–80 °C), and it was redissolved in NMP. It was reprecipitated with petroleum ether and was dried in vacuum at 40 °C. It was then washed repeatedly with water to leach out any trace of Cu^+ ion present in the polymer.

The lithium triflate (LiCF_3SO_3) was doped in the above made PD graft copolymer by mixing the appropriate amounts of lithium triflate solutions with the solution of PD graft copolymer in *N,N'*-dimethyl formamide (DMF). They were evaporated to dryness in a petridish and finally in vacuum. The samples are designated as PDLi1 and PDLi5 for 1% and 5% (w/w) Li^+ ion doping.

FT-IR spectra of the samples were obtained from thin films cast from DMF solutions on a silicon wafer using a Perkin-Elmer FT-IR instrument (spectrum100). The X-ray data are taken from DMF cast films using a Bruker AXS diffractometer (model D8 Advance) using a Lynx Eye detector. The instrument is operated at a 40 KV voltage and at a 40 mA current. The sample is scanned in the range $2\theta = 2^\circ$ to 35° at the scan rate of 0.5 s/step with a step width of 0.02° .

For impedance measurements, we used a Solartron SI 1260 impedance analyzer (Solartron, U.K.) fitted with DNHT liquid nitrogen cryostat (Oxford Instruments, U.K.). The sample films (thickness ≈ 0.1 mm, and diameter = 8–11 mm) were connected through connecting wires of the impedance meter using Ag paste. The probe was then carefully inserted into the thermostat and was made vacuum, where a small He gas was introduced to

maintain the thermal homogeneity. Liquid N_2 is used as a coolant of the thermostat.

Two types of experiments were performed. In the frequency sweep experiment, the impedance measurements were carried out at 30 °C over the frequency range $1\text{--}10^6$ Hz for an oscillation voltage of 100 mV at 0 V DC level. The AC conductivity of the system was calculated from the relation $\epsilon'' = G_p t / \omega \epsilon_0 A$ where G_p is the conductance, t is the sample thickness, A is the sample area, ϵ_0 is the free space dielectric permittivity, ϵ'' is the relative permittivity (imaginary part), and $\omega = 2\pi f$ is the angular frequency. In the temperature ramp experiment, the impedance

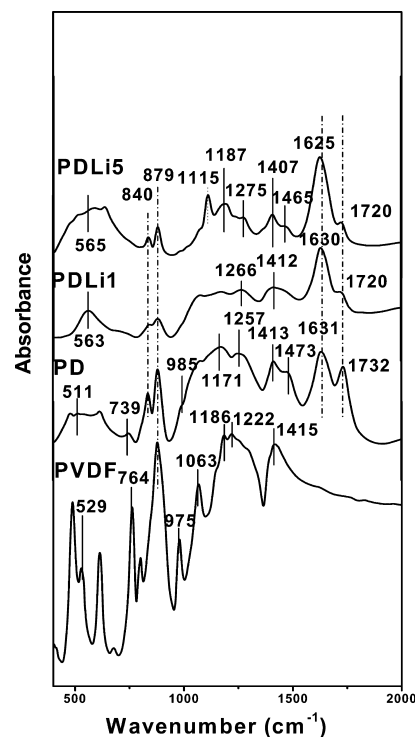


Figure 1. FTIR spectra of PVDF, PD, PDLi1, and PDLi5.

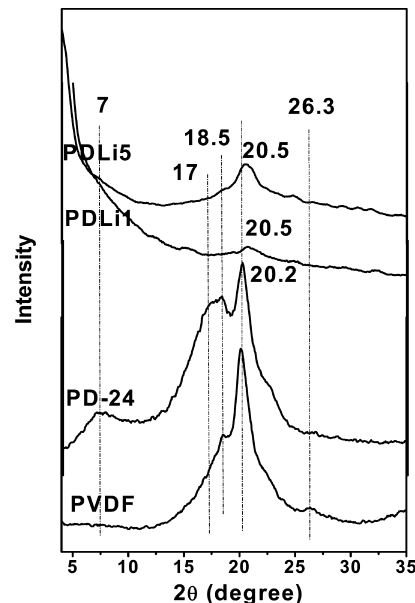


Figure 2. WAXS spectra of PVDF, PD-24, PDLi1, and PDLi5.

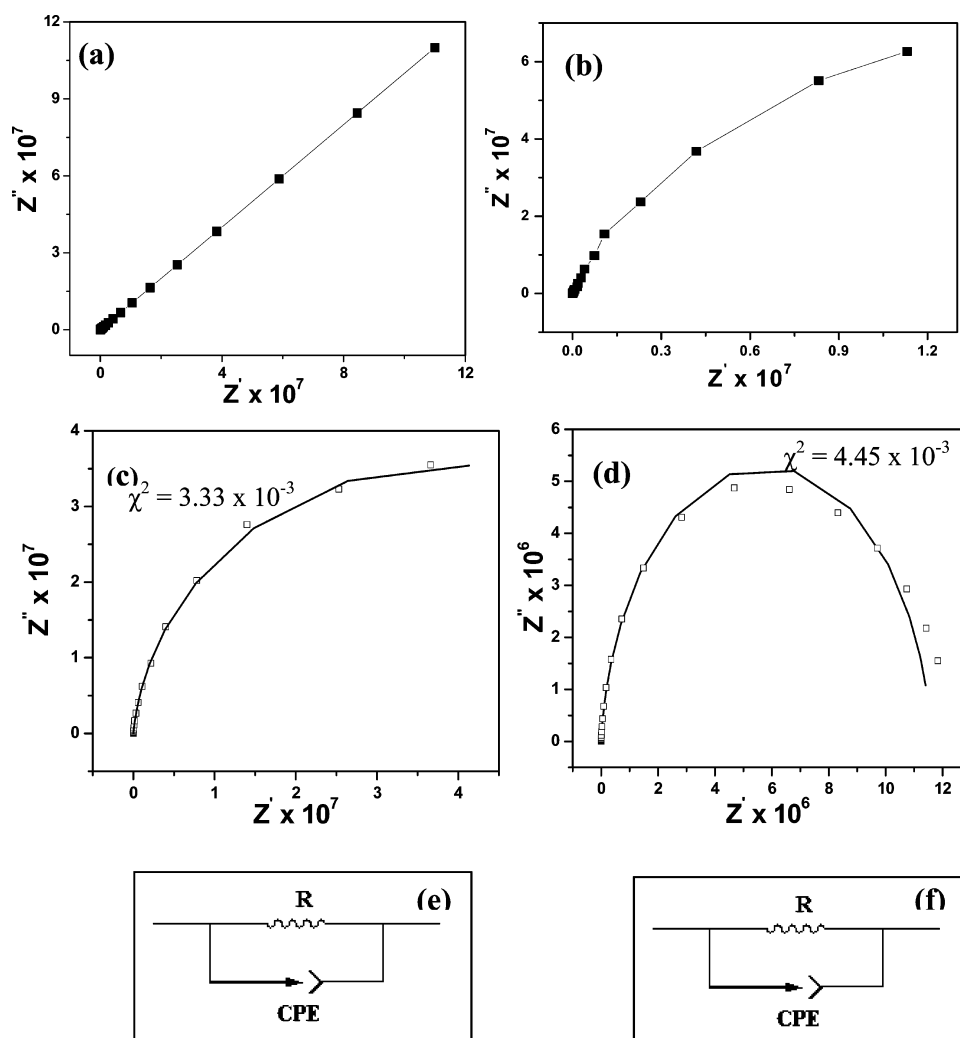


Figure 3. Impedance spectra for (a) PVDF and (b) PDMAEMA and fitting curves of (c) PDLi1% and (d) PDLi5% with the indicated fitting parameters and equivalent R–C circuit with constant phase element of (e) PDLi1% and (f) PDLi5%.

was measured at a constant frequency of 5 Hz at a scanning rate of 5 °C/min.

RESULTS AND DISCUSSION

There are numerous $>\text{C}=\text{O}$ groups in the grafted PDMAEMA chain of the PD graft copolymer. The $>\text{C}=\text{O}$ groups could stabilize the Li^+ ions by coordination, and it is supported from the FTIR spectra (Figure 1) where the $>\text{C}=\text{O}$ stretching peak at 1732 cm^{-1} has shifted to lower energy (1720 cm^{-1}). Also the relative intensity of this peak is greatly reduced indicating the ion–dipolar interaction of Li^+ ion by $>\text{C}=\text{O}$ groups of grafted DMAEMA chains. It is interesting to note that the structure of PVDF, which crystallizes in α -polymorph character (having characteristic FTIR peaks at 975 , 764 , and 529 cm^{-1})¹⁷ in the neat polymer, exhibits a mixture of α and β phase formation in the PD graft copolymer,² the latter being characterized by 511 and 840 cm^{-1} . However, the characteristic peak of β polymorph at 1272 cm^{-1} is not clearly observed, probably due to the broadness of absorption, and it appears at 1257 cm^{-1} . In PDLi1 and PDLi5 samples, the peaks at $840/1266$ and $840/1275\text{ cm}^{-1}$ are clearly observed, respectively. The presence of 1266 and 1275 cm^{-1} peaks certainly indicate the β phase formation^{17a–f} in the above polymer electrolytes; however, no absorption peak at 975 , 764 , and 529 cm^{-1} corresponding to α phase PVDF for PDLi1

and PDLi5 is observed. We may therefore infer that Li^+ ion gradually induces reorganization of PVDF chains from TGTG' conformation of α phase to the all trans β conformation in the PD graft copolymer, and it is complete in the PDLi5 sample.

The WAXS spectrum of PVDF exhibits peaks at $2\theta = 18.5$, 20.2 , and 26.3° (Figure 2) characterizing the formation of α -polymorph,^{17c,18a–d} and it is also supported from the FTIR spectra discussed above. In the WAXS pattern of the PD graft copolymer, the lower angle peak at $2\theta = 7^\circ$ is broad, which suggests the formation of a highly dispersed self-organized short-range ordering produced from the supramolecular interactions between tertiary amine N atom, $>\text{C}=\text{O}$ group, and $>\text{CF}_2$ groups.² In the PD graft copolymer, the diffraction peaks at 18.5 , 20.2 , and 26.3° are present with a lower relative intensity of the 26.3° peak, suggesting a mixture of α and β polymorph formation. It is important to note that the WAXS pattern of PDLi1 and PDLi5 samples are completely different from those of PVDF and PD graft copolymers. Here, only one diffraction peak at $2\theta = 20.5^\circ$ is observed characterizing the formation of β polymorph and supporting the FTIR observation discussed above. Also, the diffraction peak at $2\theta = 7^\circ$ is lost probably due to the loss of supramolecular ordering in the PD graft copolymer. One probable explanation is that the Li^+ coordinates with the $>\text{C}=\text{O}$ group,³ thus reducing the interaction between $>\text{C}=\text{O}$

and $>\text{CF}_2$ groups of PVDF, and it is also evidenced from the FTIR spectra (Figure 1) where the relative intensity of $>\text{C}=\text{O}$ stretching peak at 1720 cm^{-1} with respect to 1631 cm^{-1} peak (I_{1720}/I_{1631}) is greatly reduced (the 1631 cm^{-1} peak corresponds to the C–N stretching vibration of PD copolymer corresponding to it is dimethyl amino group). Thus, both the WAXS and FTIR results support the formation of β polymorph PVDF in the Li^+ -doped PD samples, and this may be attributed to the ion–dipolar interaction between the Li^+ ions and the $>\text{CF}_2$ dipoles of PD graft copolymer. This dipolar interaction causes stretching of the PVDF chain facilitating the crystallization in β polymorph as β PVDF is normally produced under the stretched conditions.^{19a,b} Another mechanism of the β PVDF formation is the crystallization of PVDF on the nanoparticle surface where the adsorption energy overcomes the potential energy required for β phase formation.^{20a–f} In the present system, however, it is better explained from the extension of the chain due to dipolar attraction that causes β phase PVDF formation.

An important method for the nondestructive electrical characterization of the materials is the ac-impedance analysis of the samples. In order to analyze and interpret the experimental results, a model equivalent circuit is required and a primary idea of it can be obtained from the Nyquist plot where the imaginary part of impedance (Z'') is plotted with real part (Z') representing a typical Cole–Cole plot in the complex impedance plane. In Figure 3, such plots for PVDF, PD, PDLi1, and PDLi5 samples at 298 K are presented. From Figure 3a, it is evident that the Z'' vs Z' plot of PVDF is purely linear, suggesting the resistance of the sample is very high. In the PD graft copolymer (Figure 3b), a curvature has appeared indicating a decrease of its resistance due to grafting with PDMAEMA. It may be attributed to the different π -electrons present in the grafted PDMAEMA chains and also due to the supramolecular interactions, which increase the charge carrier mobility in the polymer matrix due to partial delocalization. On doping the PD graft copolymer with Li^+ (1%) (Figure 3c), the curvature further increases, but it fails to produce the semicircle, which is completed in 5% Li^+ doping (Figure 3d). In order to interpret the plot of Figure 3d, an equivalent circuit model, which signifies the existence of both resistive (R) and capacitive (C) features in the material connected in a parallel mode, is required.^{21,22} We have fitted the impedance spectra (Figure 3) of PDLi1 and PDLi5 samples from the Z-view program (Solartron, U.K.), and the corresponding resistance and capacitance values are calculated. The resistance of PDLi1 is $78\text{ M}\Omega$, and capacitance with constant phase element (CPE) is equal to 1.38 nF having a phase angle of 0.94 . For PDLi5 sample, the resistance is $16.1\text{ M}\Omega$, and $\text{CPE} = 1.46\text{ nF}$ with the same phase angle as the former. So an increase of Li^+ concentration in the PD graft copolymer causes a significant decrease of Ohmic resistance with a small increase of capacitance. A typical Cole–Cole plot is also observed in the Modulus plane plots of the PDLi1 and PDLi5 samples (Figure 4) showing only one peak. It is necessary to mention here that the Z'' vs Z' plot of PDLi1 sample does not exhibit any peak, but the appearance of only one peak in the complex modulus planes (Figure 4) supports the presence of only one equivalent circuit in both PDLi1 and PDLi5 samples as evident from the fitted curves.

In Figure 5, the spectroscopic plot of the imaginary component (Z'') vs frequency are shown for all the samples. Pure PVDF does not exhibit any peak, but the other three samples exhibit one Debye peak. It becomes more prominent with increasing Li^+ concentration, and PDLi5 sample has the

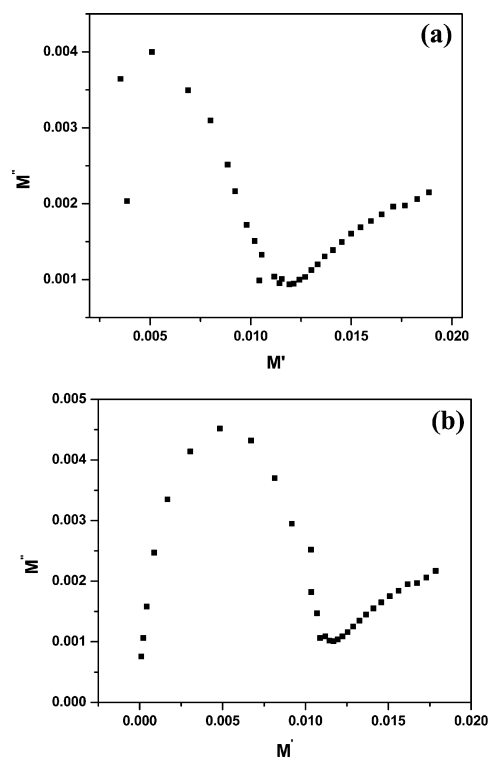


Figure 4. Modulus plane plots for (a) PDLi1% and (b) PDLi5%.

most prominent Debye peak. The Debye peak in the imaginary Modulus component (M'') vs frequency plots is also observed in the doped samples (Figure 6), and here also, the peak is prominent in the PDLi5 sample. A single Debye peak in both Z'' and M'' spectroscopic plots (Figures 5 and 6) indicates an almost isotropic behavior of the samples, and the impedance response in the PDLi5 sample can be represented by an equivalent parallel resistance–capacitance (R – C) circuit. It is to be noted here that the PD graft copolymer exhibits a Debye peak in the spectroscopic plot of Z'' vs frequency, but it is not observed in M'' vs frequency plot, and it may be attributed to the very high resistance of the sample.

The ac-conductivity of all the samples is plotted with angular frequency (Figure 7), and it is apparent from the plot that the ac-conductivity increases almost linearly with angular frequency in PVDF and PDMAEMA samples, but in the case of the Li^+ ion-doped samples, the nature of the plot is different. For PDLi1 sample, it remains at first constant in the frequency range $1\text{--}10^2\text{ Hz}$, and above 10^2 Hz an increase in conductivity with frequency is observed. For PDLi5 sample, it remains at first constant up to 10^3 Hz , and above 10^3 Hz , an increase in conductivity with frequency is observed.

The conductivity–frequency spectral data of PDLi1 and PDLi5 samples can be explained from the jump relaxation model (JRM).²³ The frequency-independent conductivity at the low frequency region is attributed to the successful hops of Li^+ ions to its neighboring vacant site for the long time period of vibration contributing to the dc-conductivity. At the intermediate frequency region ($10^2\text{--}10^4\text{ Hz}$), two competing transport processes occur: (i) the jumping ion jumps back to its initial position, i.e., an unsuccessful hopping, and (ii) as a result, the neighboring ions relax in a new site, i.e., a successful hopping. The increased ratio of successful to unsuccessful hopping causes a rise in conductivity at this frequency range. Hence,

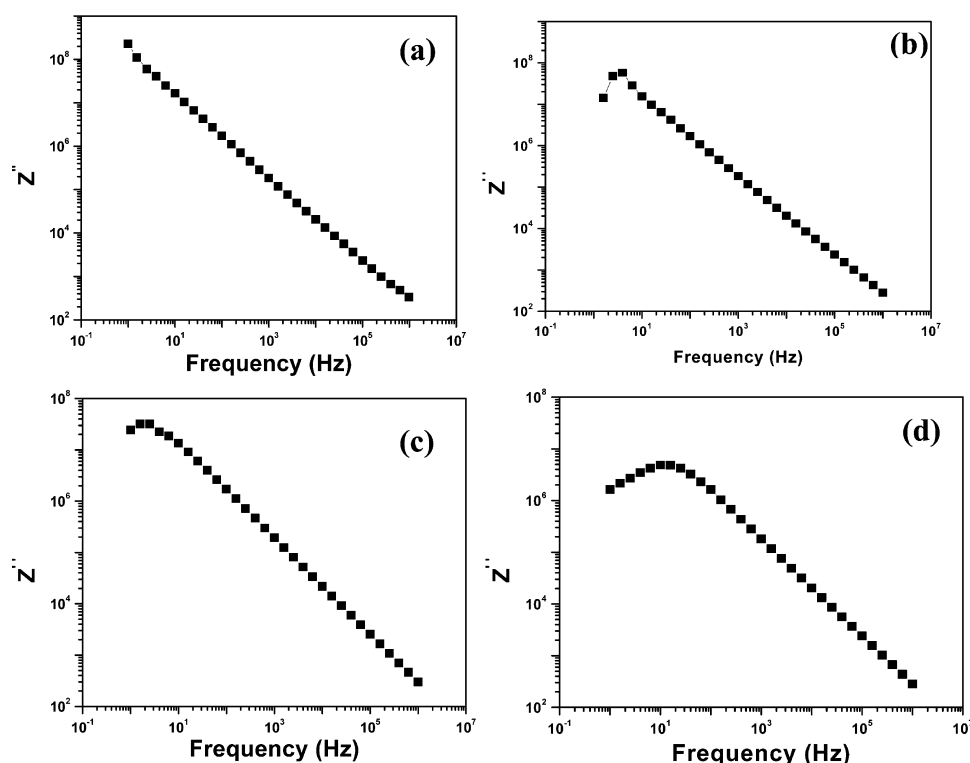


Figure 5. Impedance Z'' (imaginary) spectroscopic plots against frequency for (a) PVDF, (b) PDMAEMA, (c) PDLi1%, and (d) PDLi5%.

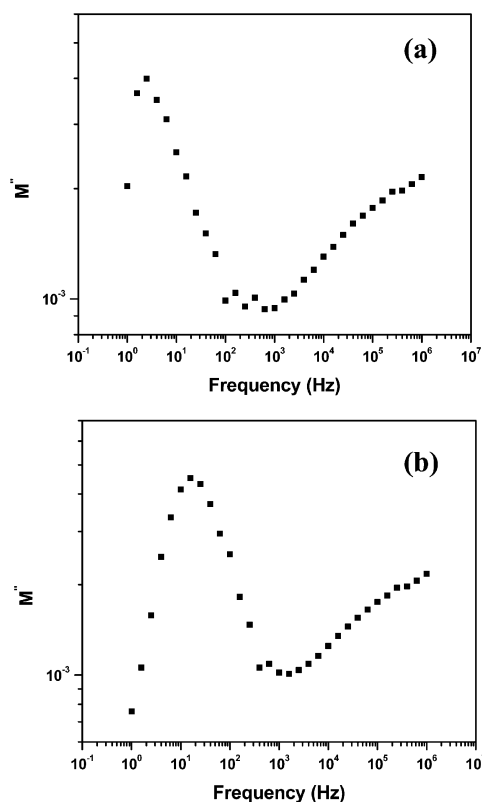


Figure 6. Modulus M'' (imaginary) spectroscopic plots against frequency for (a) PDLi1% and (b) PDLi5%.

the frequency dependency of ac-conductivity [$\sigma(\omega)$] has been expressed as²⁴

$$\sigma(\omega) = \sigma(0) + A\omega^n \quad (\text{i})$$

where $\sigma(0)$ is the frequency-independent conductivity, A is a coefficient, and n is an exponent that depends on the intrinsic property of the sample and temperature. For frequency $>10^5$ Hz, the above power-law can be extended to the double power law²⁵

$$\sigma(\omega) = \sigma(0) + A_1\omega^{n_1} + A_2\omega^{n_2} \quad (\text{ii})$$

where the first two terms have the same meaning as eq (i) and the last term of eq (ii) corresponds to reorientational (localized) hopping that occurs for the very low time period motion. Therefore, the variation of $\sigma(\omega)$ with frequency may be attributed to three different regions as marked in the figure. In region 1, long-range translational hopping of Li^+ occurs, in region 2, the exponent ($0 < n_1 < 1$) corresponds to short-range translational hopping. By standard fitting of the data, we find that $n_1 = 0.92$ in this system. In region 3, the exponent lies in the range $0 < n_2 < 2$, corresponding to the reorientational (localized) hopping,²⁶ and the standard fitting of the data suggests $n_2 = 1.5$. Thus, the frequency dependency of conductivity is well explained from the double power-law giving an insight of the conduction mechanism.

The temperature dependency of ac-conductivity of all the samples is shown in Figure 8 at the temperature range of 298–398 K. The conductivity of PVDF is almost independent of temperature (Figure 8a) indicating insulating character, whereas that of PDMAEMA decreases with increase in temperature indicating metallic character. The conductivity of PDLi1 slightly increases initially and then decreases, and that of PDLi5 shows a prominent increase initially and then decreases with rise in temperature. The results indicate a semiconducting behavior at lower temperature, and at higher temperature, it exhibits metallic behavior. PVDF is a highly insulating polymer, and activation energy is so large that, in the experimental temperature range, it practically shows a temperature independent ac-conductivity. In the PD graft copolymer, the conductivity is about one order

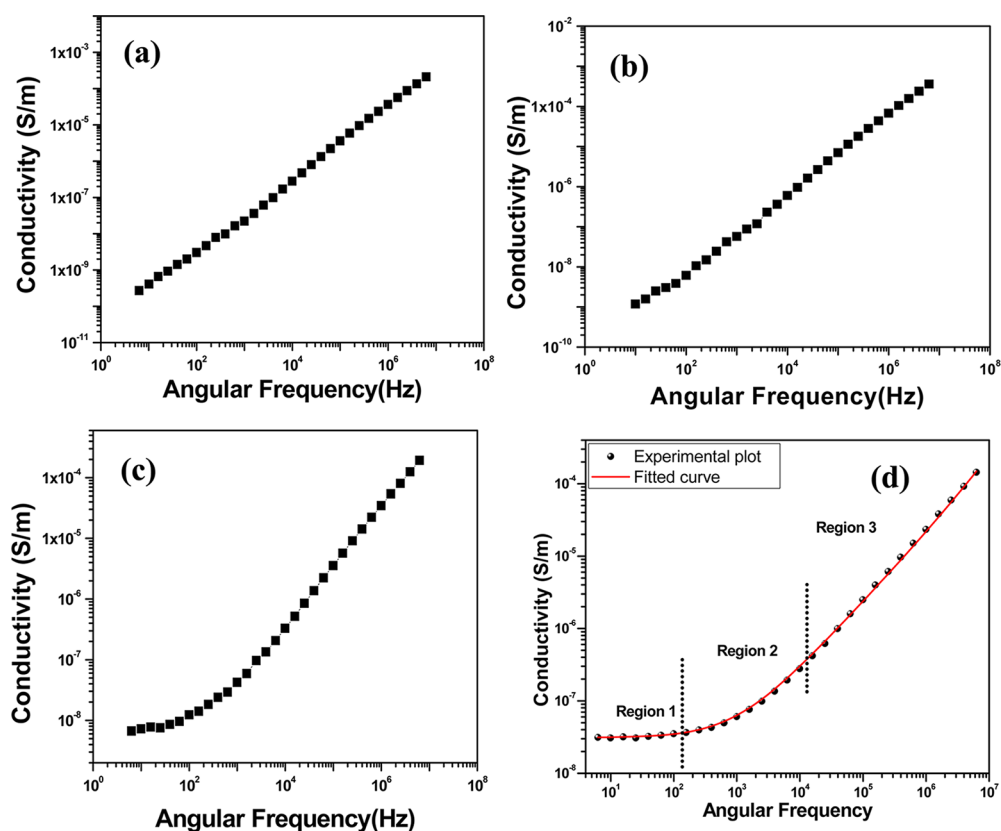


Figure 7. Plot of ac-conductivity against frequency for (a) PVDF, (b) PDMAEMA, (c) PDLi1%, and (d) PDLi5%.

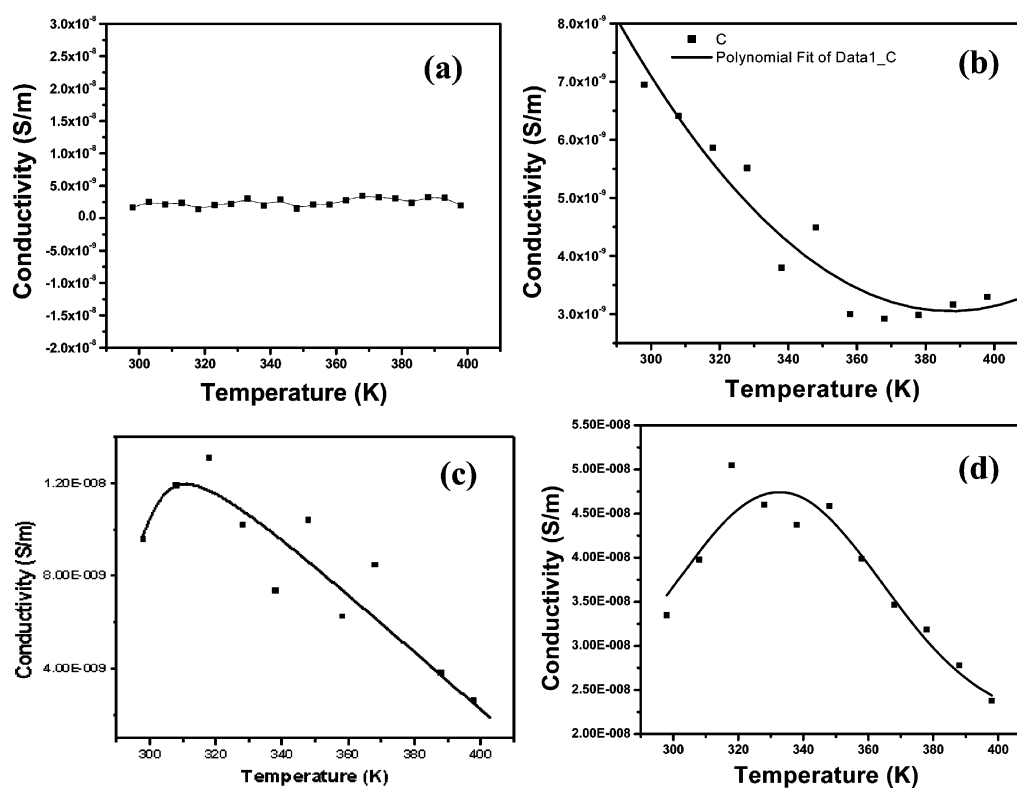


Figure 8. Plot of conductivity against temperature for (a) PVDF, (b) PDMAEMA (polynomial fit according to the equation $y = A + B_1x + B_2x^2$, where $A = 8.27 \pm 1.86 \times 10^{-8}$, $B_1 = -4.12 \pm 1.08 \times 10^{-10}$, $B_2 = 5.31 \pm 1.55 \times 10^{-13}$), (c) PDLi1%, and (d) PDLi5%.

higher than that of PVDF at 300 K, but with increase of temperature, the conductivity decreases. In the PD graft copolymer, loop-like microstructures are produced in plenty

due to the presence of supramolecular interaction (e.g., dipole–dipole, ion–dipole, H-bonding, etc.),² and this causes a partial delocalization of electrons showing higher conductivity. With

increase of temperature, these H-bonds gradually break, abolishing the loop-like microstructure. This decreases the delocalization of electrons, and hence, conductivity decreases until a leveling value is reached at 3×10^{-9} S/m, which is close to that of pure PVDF. With the addition of 1% Li^+ , the conductivity shows a higher value than that of PD graft copolymer, and with increase of temperature, it first increases and then gradually decreases. In the case of 5% Li^+ , the increase in conductivity with increase of temperature is relatively higher showing a maximum at ~ 335 K, and then, it decreases sharply. The increase of conductivity with increase of temperature may be attributed to the increasing mobility of Li^+ with temperature, but the breaking of supramolecular bonding (between $>\text{C}=\text{O}$ and $>\text{CF}_2$ and $>\text{C}=\text{O}$ and Li^+) with temperature causes the conductivity to decrease. Because of these two opposite effects, a maximum is reached, and above 335 K, the decreasing part becomes prominent. Hence, the variation of conductivity with temperature for Li^+ -doped PD graft copolymer is complex in nature, and both the ionic contribution and supramolecular contribution of conductivity operate in opposite manner with increase of temperature.

We made a temperature-dependent FTIR spectral study of PDLi1 and PDLi5 samples (Figures 9 and 10) to understand any

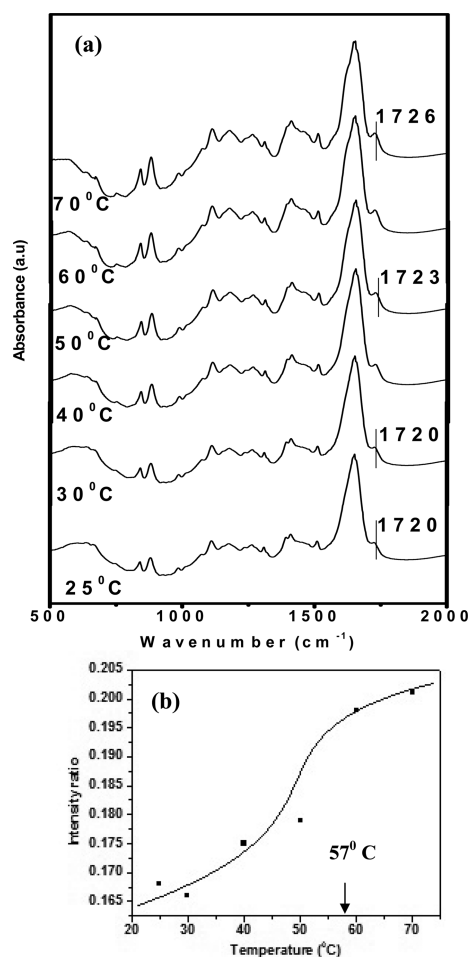


Figure 9. (a) Temperature-dependent FTIR of PDLi5% and (b) plot of I_{1720}/I_{1631} against temperature ($^{\circ}\text{C}$).

change of supramolecular interaction between $>\text{C}=\text{O}$ and $>\text{CF}_2$; $>\text{CF}_2$ and Li^+ ; and $>\text{C}=\text{O}$ and Li^+ with increase of

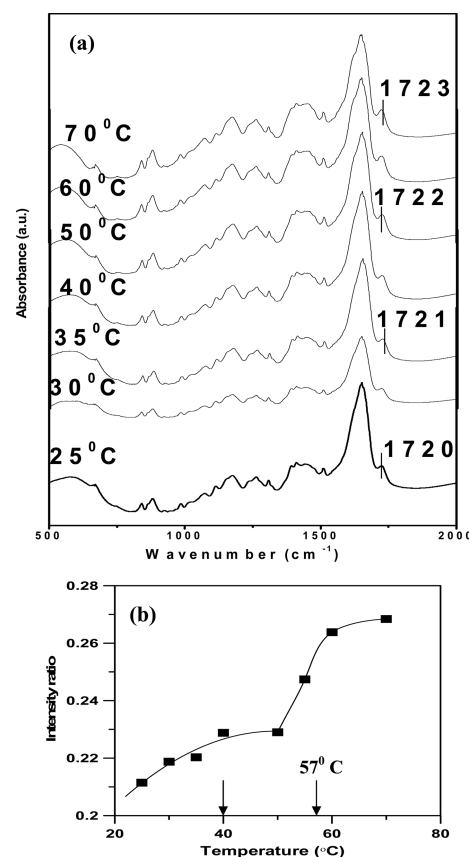


Figure 10. (a) Temperature-dependent FTIR of PDLi1% and (b) plot of I_{1720}/I_{1631} against temperature ($^{\circ}\text{C}$).

temperature. From Figure 9a, it is apparent that the 1720 cm^{-1} peak of the $>\text{C}=\text{O}$ group shows a gradual shift to 1726 cm^{-1} for increase of temperature from 25 to $70\text{ }^{\circ}\text{C}$ in the PDLi5 sample. This shift to higher energy is due to the breaking of a supramolecular interaction causing the $>\text{C}=\text{O}$ bonding electrons to become more localized and hence requires more energy for the stretching vibration. The absorbance ratio of 1720 and 1631 cm^{-1} absorption peaks (I_{1720}/I_{1631}) shows a sigmoidal rise with increase in temperature (Figure 9b), and it may be attributed to the breaking of supramolecular interaction causing an increase in transition probability of $>\text{C}=\text{O}$ vibration as it is evident from the discussion on Figure 1 where, upon addition of Li^+ , the relative intensity of $>\text{C}=\text{O}$ stretching peak at 1720 cm^{-1} with respect to 1631 cm^{-1} peak has greatly reduced. The sigmoidal nature of the curve reflects the cooperative nature of the annihilation process, and it is completed at $57\text{ }^{\circ}\text{C}$ for the PDLi5 sample. This temperature almost equals the maximum of the conductivity vs temperature plot from where a large decrease in conductivity of the sample occurs. For PDLi1 sample (Figure 10a), the vibration band of the $>\text{C}=\text{O}$ group shows a gradual shift from 1720 to 1723 cm^{-1} indicating breaking of supramolecular interaction as discussed above, and the shift is much lower than that of PDLi5 sample suggesting a weaker interaction in PDLi1 sample. The plot of intensity ratio (I_{1720}/I_{1631}) with temperature (Figure 10b) of this sample, however, exhibits two breaks. The exact reason of the two breaks is not known and may characterize the breaking of two different types of supramolecular linkages, e.g., (i) the dipolar interaction between $>\text{C}=\text{O}$ and $>\text{CF}_2$ and (ii) the ion–dipolar interaction between $>\text{C}=\text{O}$ and Li^+ and $>\text{CF}_2$ and Li^+ . The ion–dipolar

interaction would be stronger than the former due to the stronger attraction of Li^+ ion; hence, in PDLi5, due to the larger concentration of Li^+ , the initial break is not observed. The first inflection is complete at 40 °C, and the second inflection is complete at 57 °C; however, the former inflection corresponds to the maximum in the conductivity–temperature plot because of very low concentration of Li^+ in the PDLi1 sample. Thus, these results conclude that both the ionic part and supra-molecular part contribute to the total conductivity of PDLi1 and PDLi5 samples.

CONCLUSIONS

It is evident from the FTIR and WAXS study that, in the PD graft copolymer, the α polymorph of PVDF changes to a mixture of α and β polymorph and that it transforms to purely piezoelectric β polymorph on doping with 1% (w/w) Li^+ ion. The impedance of PVDF changes on grafting, and that of the PD graft copolymer also changes with an increase in Li^+ ion dopant concentration. In the Z'' vs Z' plot (Nyquist plot), PVDF exhibits a straight line character, and in the PD graft copolymer, a curvature has appeared. On doping the latter with Li^+ ion (1% w/w), the curvature increases, and a semicircle is completed on 5% Li^+ ion doping due to a gradual decrease of resistance. Fitting the data from the Z-view program, the Ohmic resistance of PDLi1 is found to be 78 M Ω having capacitance with constant phase element (CPE) = 1.38 nF, while for the PDLi5 sample, the resistance decreases to 16.1 M Ω and CPE shows a small increase to 1.46 nF. Modulus plane plots for PDLi1 and PDLi5 samples also exhibit only one peak supporting the presence of only one equivalent circuit in both PDLi1 and PDLi5 samples. Both the impedance and modulus vs frequency plots of PDLi1 and PDLi5 samples exhibit a single Debye peak indicating the isotropic nature of the samples. PVDF and PDMAEMA samples exhibit a linear increase of ac-conductivity with angular frequency, but in the case of PDLi1 and PDLi5 samples, it is invariant in the frequency range 1–10² Hz, and above 10² Hz, a curvilinear increase in conductivity with frequency occurs. The variation of conductivity with frequency is explained from the double power law, contributed from three different transport processes, e.g., (i) successful hopping of Li^+ ions to its neighboring vacant site at low frequency contributing to the dc-conductivity, (ii) at intermediate frequency region, a jumping ion jumps back to its initial position resulting in the neighboring ions to relax in a new site, causing a successful hopping, and (iii) at higher frequency, conductivity arises from reorientational (localized) hopping. PVDF exhibits insulating character in the temperature variation of conductivity, but in the PD graft copolymer, the conductivity decreases with increase of temperature (metallic-like behavior) due to the breaking of supra-molecular interaction. The temperature variation of conductivity in the Li^+ -doped PD graft copolymer suggests that both the ionic contribution and supra-molecular contribution of conductivity operate in opposite manner; the former increases, while the latter decreases, showing a maximum with increase in temperature. The temperature-dependent FTIR spectra of PDLi1 and PDLi5 samples support the gradual breaking of supra-molecular interaction with an increase of temperature.

AUTHOR INFORMATION

Corresponding Author

*E-mail: psuakn@iacs.res.in.

Notes

The authors declare no competing financial interest.

ACKNOWLEDGMENTS

We gratefully acknowledge Department of Science and Technology, New Delhi (Grant No. SR/SI/PC-26/2009) for financial support of the work. A.K. acknowledges CSIR, New Delhi, for providing the fellowship.

REFERENCES

- (1) Nasongkla, N.; Bey, E.; Ren, J.; Ai, H.; Khemtong, C.; Guthi, J. S.; Chin, S. F.; Sherry, A. D.; Boothman, D. A.; Gao, J. *Nano Lett.* **2006**, *6*, 2427–2430.
- (2) Samanta, S.; Chatterjee, D. P.; Manna, S.; Mandal, A.; Garai, A.; Nandi, A. K. *Macromolecules* **2009**, *42*, 3112–3120.
- (3) Samanta, S.; Chatterjee, D. P.; Layek, R. K.; Nandi, A. K. *Macromol. Chem. Phys.* **2011**, *212*, 134–149.
- (4) Rahane, S. B.; Hensarling, R. M.; Sparks, B. J.; Stafford, C. M.; Patton, D. L. *J. Mater. Chem.* **2012**, *22*, 932–943.
- (5) Gadjourova, Z.; Andreev, Y. G.; Tunstall, D. P.; Bruce, P. G. *Nature* **2001**, *412*, 520–523.
- (6) Liivat, A.; Brandell, D.; Aabloo, A.; Thomas, J. O. *Polymer* **2007**, *48*, 6448–6456.
- (7) Itoh, T.; Miyamura, Y.; Ichikawa, Y.; Uno, T.; Kubo, M.; Yamamoto, O. *J. Power Sources* **2003**, *119*, 403–408.
- (8) Meyer, W. H. *Adv. Mater.* **1998**, *10*, 439–448.
- (9) Karmakar, A.; Ghosh, A. *Curr. Appl. Phys.* **2012**, *12*, 539–543.
- (10) Karmakar, A.; Ghosh, A. *Phys. Rev. E* **2011**, *84*, 051802 1–9.
- (11) Karmakar, A.; Ghosh, A. *J. Appl. Phys.* **2010**, *107*, 104113 1–6.
- (12) Dias, F. B.; Plomp, L.; Veldhuis, J. B. J. *J. Power Sources* **2000**, *88*, 169–191.
- (13) Wang, X.; Xiao, P. *J. Eur. Ceram. Soc.* **2000**, *20*, 2591–2599.
- (14) Sinclair, D. C.; West, A. R. *J. Appl. Phys.* **1989**, *66*, 3850–3856.
- (15) Karmakar, A.; Ghosh, A. *J. Appl. Phys.* **2011**, *110*, 034101 1–6.
- (16) (a) McDonald, J. R., Ed. *Impedance Spectroscopy Emphasizing Solid Materials and Systems*; John Wiley & Sons: New York, 1987. (b) Mukherjee, P.; Nandi, S.; Nandi, A. K. *Synth. Met.* **2012**, *162*, 904–911.
- (17) (a) Cortili, G.; Zerbi, G. *Spectrochim. Acta, Part A* **1967**, *23*, 2216–2218. (b) Tashiro, K.; Kobayashi, M.; Tadokoro, H. *Macromolecules* **1981**, *14*, 1757–1764. (c) Tashiro, K.; Kobayashi, M. *Phase Trans.* **1989**, *18*, 213–246. (d) Mandal, A.; Nandi, A. K. *J. Phys. Chem. C* **2012**, *116*, 9360–9371. (e) Priya, L.; Jog, J. P. *J. Polym. Sci., Part B: Polym. Phys.* **2002**, *40*, 1682–1689. (f) Shah, D.; Maiti, P.; Gunn, E.; Schmidt, D. F.; Jiang, D. D.; Batt, C. A.; Giannelis, E. P. *Adv. Mater.* **2004**, *16*, 1173–1177.
- (18) (a) Lando, J. B.; Doll, W. W. *J. Macromol. Sci. Phys.* **1968**, *B-2*(2), 205–218. (b) Hasagawa, R.; Takahashi, Y.; Chatani, Y.; Tadokoro, H. *Polym. J.* **1972**, *3*, 600–610. (c) Bachmann, M. A.; Lando, J. B. *Macromolecules* **1981**, *14*, 40–46. (d) Guerra, G.; Karasz, F. E.; MacKnight, W. J. *Macromolecules* **1986**, *19*, 1935–1938.
- (19) (a) Du, C. H.; Zhu, B. K.; Xu, Y. Y. *J. Appl. Polym. Sci.* **2007**, *104*, 2254–2259. (b) Chang, W. Y.; Fang, T. H.; Liu, S. Y.; Lin, Y. C. *Mater. Sci. Eng., A* **2008**, *480*, 477–482.
- (20) (a) Yu, S. S.; Zheng, W. T.; Yu, W. X.; Zhang, Y. J.; Jiang, Q.; Zhao, Z. *Macromolecules* **2009**, *42*, 8870–8874. (b) Mandal, A.; Nandi, A. K. *J. Phys. Chem. C* **2012**, *116*, 9360–9371. (c) Manna, S.; Nandi, A. K. *J. Phys. Chem. C* **2007**, *111*, 14670–14680. (d) Layek, R. K.; Samanta, S.; Chatterjee, D. P.; Nandi, A. K. *Polymer* **2010**, *51*, 5846–5856. (e) Manna, S.; Batabyal, S. K.; Nandi, A. K. *J. Phys. Chem. B* **2006**, *110*, 12318–12326. (f) Manna, S.; Nandi, A. K. *J. Phys. Chem. B* **2011**, *115*, 12325–12326.
- (21) (a) Kalpana, D.; Renganathan, N. G.; Pitchumani, S. *J. Power Sources* **2006**, *157*, 621–623. (b) Campbell, A. J.; Bradley, D. D. C.; Lidzey, D. G. *J. Appl. Phys.* **1997**, *82*, 6326–6342.
- (22) Hui, D.; Alexandrescu, R.; Chipara, M.; Morjan, I.; Aldica, G.; Chipara, M. D.; Lau, K. T. *J. Optoelectron. Adv. Mater.* **2004**, *6*, 817–824.
- (23) Funke, K. *Prog. Solid State Chem.* **1993**, *22*, 111–195.

- (24) Jonscher, A. K. *Nature* **1975**, 253, 717–719.
- (25) Barranco, A. P.; Amador, M. P. G.; Huanosta, A.; Valenzuela, R. *Appl. Phys. Lett.* **1998**, 73, 2039–2041.
- (26) Ortega, N.; Kumar, A.; Bhattacharya, P.; Majumder, S. B.; Katiyar, R. S. *Phys. Rev. B* **2008**, 77, 014111 1–10.